Pilot-Free Polar-Coded Communications for Short-Packet Transmission

Geon Choi
Department of Electrical Engineering
POSTECH
Pohang, South Korea
Email: geon.choi@postech.ac.kr

Namyoon Lee
Department of Electrical Engineering
POSTECH
Pohang, South Korea
Email: nylee@postech.ac.kr

***Abstract*—Conventional pilot-aided strategies for short-packet communications over fading channels suffer from spectral efficiency loss due to pilot overhead. This paper proposes a pilot-free polar-coded communication framework that eliminates explicit pilots by leveraging a code-splitting approach: information is transmitted via two polar-coded segments—a quadrature phase shift keying (QPSK)-modulated portion that enables blind channel estimation and a higher-order quadrature amplitude modulation (QAM) portion to optimize the overall code rate. Channel state information is jointly estimated during decoding using successive cancellation and the constraints imposed by polar code frozen bits. This joint channel estimation and decoding fully exploits the phase-rotation invariance of QPSK and the structure of polar codes. Once decoded, the QPSK symbols serve as implicit pilots for accurate channel estimation, which enables to perform the coherent decoding for the higher-order QAM part. Simulations over block-fading channels show the proposed pilot-free scheme achieves up to a 1 dB coding gain over pilot-aided transmission in short blocklength regimes.**

I. Introduction

Achieving ultra-reliable and low-latency communication (URLLC) for emerging applications such as autonomous driving and robot control requires highly efficient short-packet transmission. Conventional pilot-assisted transmission (PAT) allocates a fraction of each packet to pilot symbols for channel estimation, resulting in a significant loss of spectral efficiency when the packet size is small [1]–[4]. This overhead presents a fundamental bottleneck: every pilot symbol reduces the information payload, directly impacting latency and reliability. In latency-critical control systems, such as closed-loop robotics, the price of this inefficiency is magnified—every transmitted bit must count. These observations motivate the search for pilot-free communication schemes that can maintain accurate channel estimation while maximizing data throughput, thus meeting the strict demands of next-generation short-packet URLLC [5]–[10].

Polar codes have emerged as an effective coding scheme for short-packet communications, particularly following their adoption in 5G New Radio (NR) control channels. In these applications, cyclic redundancy check (CRC)-aided polar codes combined with successive cancellation list (SCL) decoding have demonstrated outstanding performance [11]–[14]. Building on this success, a range of pre-transform techniques—such as pre-transformed polar codes—have been proposed to further approach the finite blocklength capacity [15]–[21]. These advancements highlight the versatility and strong performance of polar codes in meeting the demanding requirements of URLLC.

The unique algebraic properties of polar codes open new avenues for developing non-coherent communication schemes capable of reducing or even eliminating pilot overhead [22]. Recent advances have demonstrated the potential of polar-coded blind phase estimation techniques to enhance spectral efficiency in short-packet transmission scenarios [23], [24]. Despite these promising developments, current approaches are hampered by several practical constraints. Most notably, they are largely restricted to quadrature phase shift keying (QPSK) modulation, as resolving phase ambiguities becomes significantly more challenging for higher-order constellations. Additionally, existing non-coherent schemes often require codeword lengths to be exact powers of two, limiting their flexibility and applicability in real-world systems that demand arbitrary block lengths. Finally, standard rate-matching methods, such as shortening, are difficult to employ effectively in non-coherent settings, since shortened bits lose their deterministic properties in the presence of unresolved phase ambiguities. Overcoming these limitations is crucial for realizing the full potential of non-coherent polar-coded communications in practical systems.

Motivated by the rigidity of existing non-coherent designs and the fundamental overhead of pilot-aided schemes, we propose a rate-matching and pilot-free polar-coded transmission framework. The key idea is a code-splitting architecture: a QPSK-modulated segment leverages the constant-amplitude property and algebraic structure of polar codes to enable blind channel estimation, while a higher-order quadrature amplitude modulation (QAM) segment delivers high spectral efficiency. Channel state information (CSI) and data are recovered via QPSK-modulated portion through successive cancellation decoding, jointly exploiting the constraints imposed by the frozen bits. Decoding the QPSK portion provides both information and implicit pilots, thus eliminating dedicated pilot overhead and enabling coherent detection of the QAM symbols. Simulations over block-fading channels demonstrate that the proposed pilot-free approach achieves up to a 1 dB coding gain compared to conventional pilot-aided transmission in the

short blocklength regime.

II. System Model and Background

A. System Model

We consider a communication system over a block fading channel. The channel is modeled as a scalar block-fading channel coefficient $h = |h|e^{j\phi}$, which remains constant for a packet length consisted of N_c complex symbols. Let $\mathbf{x} \in \mathbb{C}^{N_c}$ be a transmit symbol over the packet size N_c. Then, the received signal vector is given by

$$\mathbf{y} = h\mathbf{x} + \mathbf{v}, \tag{1}$$

where $\mathbf{y} \in \mathbb{C}^{N_c}$ is the received vector and $\mathbf{v} \in \mathbb{C}^{N_c}$ denotes additive white Gaussian noise (AWGN) whose elements are independent and identically distributed, i.e., $\mathbf{v} \sim \mathcal{CN}(\mathbf{0}, \sigma^2\mathbf{I})$. In this paper, we denote the ith component of the vector $\mathbf{x}$ and $\mathbf{x}_k$ as v_i and $v_{k,i}$, respectively.

B. Pilot-Aided Communications

We begin by briefly reviewing the pilot-aided communication framework. In such systems, the transmitted symbol vector $\mathbf{x} \in \mathbb{C}^{N_c}$ is partitioned into two components: pilot symbols $\mathbf{x}_p \in \mathbb{C}^{N_p}$ and data symbols $\mathbf{x}_d \in \mathbb{C}^{N_d}$, where $N_p + N_d = N_c$. The pilot symbols, typically pseudo-random QPSK sequences of length N_p, are known a priori to the receiver and facilitate channel estimation. The data symbols, of length N_d, convey K information bits.

Assuming N_s-ary quadrature amplitude modulation (QAM) with constellation $\mathcal{X}_{N_s}$, each symbol $x_i \in \mathcal{X}_{N_s}$ represents $n_s = \log_2(N_s)$ consecutive codeword bits.[1] The constellation is normalized such that $\frac{1}{N_s}\sum_{x\in\mathcal{X}_{N_s}} |x|^2 = 1$, and Gray labeling is employed throughout [26].

Given a total packet size N_c, pilot length N_p, and modulation size N_s, the effective codeword length is $M = n_s N_d$. Accordingly, the transmitter encodes K information bits $\mathbf{m} \in \mathbb{F}_2^K$ into a codeword $\mathbf{c} \in \mathbb{F}_2^M$ with nominal code rate $R = K/M$. However, due to the pilot overhead, the effective code rate becomes

$$R_{\text{eff}}^p = \frac{K}{N_c} = \frac{K}{N_p + N_d} = (1-\alpha)n_s R, \tag{2}$$

where $\alpha = N_p/N_c$ denotes the pilot overhead fraction.

C. Polar Codes and Rate-Matching

Polar codes are defined by a transform matrix $\mathbf{F}_N = \mathbf{F}_2^{\otimes n}$ where $N = 2^n$ and $\mathbf{F}_2 = \begin{bmatrix} 1 & 0 \\ 1 & 1 \end{bmatrix}$. The code is characterized by an information index set $\mathcal{I} \subseteq \{0, 1, \ldots, N-1\}$, while the frozen index set $\mathcal{F}$ is the complement of $\mathcal{I}$. The generator matrix consists of the rows of $\mathbf{F}_N$ indexed by $\mathcal{I}$. Polar codes achieve arbitrary code rates $R = K/N$ by setting $|\mathcal{I}| = K$.

The inherent constraint of Arıkan's construction limits polar code lengths to powers of two, i.e., $M = 2^n$. To support arbitrary codeword lengths $M \neq 2^n$, rate-matching techniques are employed:

- **Shortening and Puncturing:** Used to reduce code length from a larger mother code of size $N > M$.
- **Extension and Repetition:** Used to increase code length from a smaller mother code of size $N < M$.

In 5G NR systems, quasi-uniform puncturing and shortening with sub-block interleaving are employed for rate-matching, ensuring compatibility while maintaining good performance [12]. Shortening removes the last $N-M$ interleaved codeword bits, while puncturing removes the first $N-M$ bits. Repetition extends the first $M-N$ interleaved codeword bits.

[1] We assume the codeword bits are interleaved appropriately for the bit-interleaved coded modulation (BICM) scheme [25].

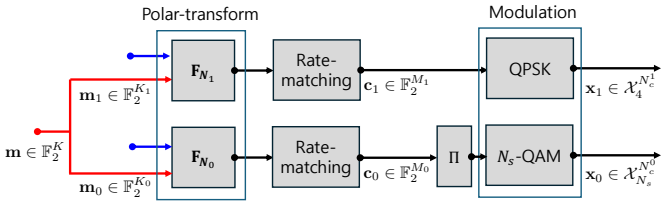

Fig. 1. Encoding structure of the proposed code-splitting method. Information bits are partitioned into two sub-messages that are independently encoded and modulated using different schemes. Π is an interleaver for BICM [25].

III. Pilot-Free Polar-Coded Modulation

In this section, we present a rate-matching, pilot-free polar-coded transmission framework designed for efficient short-packet communication over fading channels. The core of our approach is a code-splitting architecture that separates the transmission into two segments.

Consider the transmission of K information bits over N_c channel uses. The proposed scheme is parameterized by (N_c^0, N_c^1, K_0, K_1), where $N_c^0 + N_c^1 = N_c$ and $K_0 + K_1 = K$. The overall encoding structure, illustrated in Fig. 1, follows a dual-path design in which the information message $\mathbf{m} \in \mathbb{F}_2^K$ is partitioned into two sub-messages, $\mathbf{m}_0 \in \mathbb{F}_2^{K_0}$ and $\mathbf{m}_1 \in \mathbb{F}_2^{K_1}$, which are processed independently as follow:[2]

- **Component 0 (Higher-Order QAM):** The sub-message $\mathbf{m}_0$ is encoded with a polar code $\mathcal{C}_0$, resulting in a codeword $\mathbf{c}_0 \in \mathbb{F}_2^{M_0}$, with $M_0 = N_c^0 \log_2 N_s$. The codeword is mapped to N_s-QAM symbols to produce N_c^0 symbols $\mathbf{x}_0$.
- **Component 1 (QPSK for Channel Estimation):** The sub-message $\mathbf{m}_1$ is encoded with a polar code $\mathcal{C}_1$ under the constraint $\{N_1 - 2, N_1 - 1\} \subseteq \mathcal{F}_1$, yielding a codeword $\mathbf{c}_1 \in \mathbb{F}_2^{M_1}$, where $M_1 = 2N_c^1$. This codeword is QPSK-modulated to generate N_c^1 symbols $\mathbf{x}_1$.

The complete transmitted signal is $\mathbf{x} = [\mathbf{x}_0, \mathbf{x}_1]$. As a result, the effective code rate of the proposed pilot-free polar-coded transmission is thus given by

$$R_{\text{eff}} = \frac{K}{N_c} = \frac{K_0 + K_1}{N_c^0 + N_c^1} = n_s(1-\alpha)R_0 + 2\alpha R_1, \tag{3}$$

[2] The framework naturally accommodates outer codes such as CRC by treating the concatenated message $[\mathbf{m}, \mathbf{p}_{\text{crc}}]$ as the information sequence.

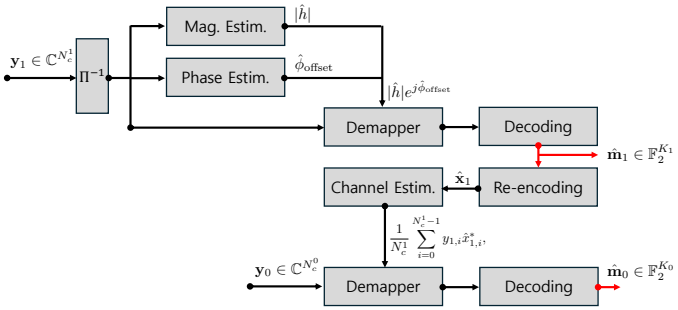

Fig. 2. Decoding flowchart showing sequential processing of QPSK and QAM portions with blind channel estimation.

where $R_i = K_i/M_i$ and $\alpha = N_c^1/N_c$.

This effective code rate formulation naturally includes the pilot-aided case as a special instance. By selecting $K_1 = 0$ and $N_c^1 = N_p$, we recover the effective code rate for conventional pilot-aided transmission, i.e., $R_{\text{eff}} = R_{\text{eff}}^p$. Thus, the proposed framework generalizes the standard pilot-aided communication system. Furthermore, by appropriately choosing the parameters (K_0, K_1, N_c^0, N_c^1), the effective code rate can be flexibly optimized to achieve a desired reliability target or spectral efficiency constraint.

In addition, the proposed method can achieve higher spectral efficiency compared to pilot-aided communication. When the decoding of $\mathbf{y}_1$ is successful, the receiver can leverage the decoded information $\hat{\mathbf{x}}_1$ for enhanced channel estimation. Since these successfully decoded symbols serve as known reference signals, they effectively function as pilot symbols while maintaining channel estimation quality equivalent to that of conventional pilot-based methods. However, unlike traditional pilot schemes where dedicated symbols carry no information, our approach enables $\mathbf{x}_1$ to simultaneously transmit data bits and provide channel estimation capability.

IV. Hybrid Decoding

In this section, we present a hybird decoding method, which decodes QPSK modulated message $\mathbf{m}_1 \in \mathbb{F}_2^{K_1}$ in a blind fassion and decodes higher-order QAM coded message bits $\mathbf{m}_0 \in \mathbb{F}_2^{K_0}$ with a coherent manner.

A. Blind Decoding for $\mathbf{x}_1$

We now describe the decoding process for $\mathbf{m}_1$, which leverages both the constant-amplitude property of QPSK modulation and the algebraic structure of polar codes. As illustrated in Fig. 2, the proposed blind decoding procedure consists of three main stages: (i) channel magnitude estimation, and (ii) channel phase estimation.

1) Channel Magnitude Estimation: For constant-amplitude modulation such as QPSK where $|x_{1,i}|^2 = 1$, channel magnitude estimation leverages the relationship

$$|y_{1,i}|^2 = |h|^2|x_{1,i}|^2 + |v_{1,i}|^2 + 2\mathsf{Re}(h^* x_{1,i}^* v_{1,i}). \tag{4}$$

Since the noise components $v_{1,i}$ are i.i.d. with zero mean, averaging over all received symbols yields

$$\frac{1}{N_c^1}\sum_{i=0}^{N_c^1-1}|y_{1,i}|^2 \approx |h|^2 + \sigma^2, \tag{5}$$

providing the magnitude estimate

$$|\hat{h}| = \sqrt{\max\left(0, \frac{1}{N_c^1}\sum_{i=0}^{N_c^1-1}|y_{1,i}|^2 - \sigma^2\right)}, \tag{6}$$

where the $\max(\cdot, 0)$ operation ensures non-negative estimates in the presence of estimation errors.

2) Channel Phase Estimation: Channel phase estimation is more challenging due to the rotational symmetry inherent in QPSK modulation. The channel phase $e^{j\phi}$ rotates all received symbols by ϕ radians. However, the four-fold rotational symmetry of QPSK creates an inherent ambiguity in phase estimation, as rotations by multiples of $\pi/2$ cannot be distinguished without additional information.

Due to this phase ambiguity, the estimated phase $\hat{\phi}$ can be decomposed as

$$\hat{\phi} = m\frac{\pi}{2} + \hat{\phi}_{\text{offset}}, \tag{7}$$

where $m \in \{0, 1, 2, 3\}$ represents integer ambiguity and $\hat{\phi}_{\text{offset}} \in [0, \pi/2)$ is the fractional offset. We adopt the estimation strategy from [24], involving two steps: estimating the fractional offset without channel decoding, then resolving the integer ambiguity using the polar code structure.

Fractional Phase Offset Estimation: For fractional offset estimation, the method employs the Viterbi and Viterbi phase estimation (VVPE) algorithm [27]. The VVPE algorithm is designed for M-PSK modulation and operates by rotating all received symbols to a common reference point, thereby eliminating the modulation-dependent phase variations.

For QPSK ($M = 4$), the key insight is that raising each symbol to the fourth power eliminates the data-dependent phase variations:

$$4\phi = 4m\frac{\pi}{2} + 4\phi_{\text{offset}} = 4\phi_{\text{offset}}, \tag{8}$$

since $4m\pi/2 = 2m\pi$ is a multiple of 2π.

The fractional phase offset is estimated as [28]

$$\hat{\phi}_{\text{offset}} = \frac{1}{4}\tan^{-1}\left(\frac{\sum_{i=0}^{N_c^1-1}\mathsf{Im}\left(\frac{y_{1,i}^4}{|y_{1,i}|^3}\right)}{\sum_{i=0}^{N_c^1-1}\mathsf{Re}\left(\frac{y_{1,i}^4}{|y_{1,i}|^3}\right)}\right) - \frac{\pi}{4}. \tag{9}$$

Integer Phase Ambiguity Resolution: To resolve the integer ambiguity m, the approach exploits the algebraic properties of polar codes under phase rotation. Consider a polar codeword $\mathbf{c} = [c_0, c_1, c_2, c_3, \ldots, c_{N-1}]$. Phase rotations

by multiples of $\pi/2$ transform the codeword according to specific patterns:

$$\mathbf{c}^0 = [c_0, c_1, c_2, c_3, \ldots, c_{N-2}, c_{N-1}], \tag{10}$$

$$\mathbf{c}^{\pi/2} = [\bar{c}_1, c_0, \bar{c}_3, c_2, \ldots, \bar{c}_{N-1}, c_{N-2}], \tag{11}$$

$$\mathbf{c}^{\pi} = [\bar{c}_0, \bar{c}_1, \bar{c}_2, \bar{c}_3, \ldots, \bar{c}_{N-2}, \bar{c}_{N-1}], \tag{12}$$

$$\mathbf{c}^{3\pi/2} = [c_1, \bar{c}_0, c_3, \bar{c}_2, \ldots, c_{N-1}, \bar{c}_{N-2}], \tag{13}$$

where $\bar{c} = c \oplus 1$ (binary addition) and $\mathbf{c}^{\phi}$ denotes the codeword obtained after phase rotation by ϕ.

These transformations can be decomposed into a permutation followed by a translation. The permutation σ is defined as

$$\sigma : [c_0, c_1, c_2, c_3, \ldots] \mapsto [c_1, c_0, c_3, c_2, \ldots], \tag{14}$$

which swaps adjacent pairs of bits. The rotated codewords can then be expressed as

$$\mathbf{c}^{\pi/2} = \sigma(\mathbf{c}^0) \oplus [1, 0, 1, 0, \ldots, 1, 0], \tag{15}$$

$$\mathbf{c}^{\pi} = \sigma(\mathbf{c}^0) \oplus [1, 1, 1, 1, \ldots, 1, 1], \tag{16}$$

$$\mathbf{c}^{3\pi/2} = \sigma(\mathbf{c}^0) \oplus [0, 1, 0, 1, \ldots, 0, 1], \tag{17}$$

where $\oplus$ denotes bit-wise XOR operation.

According to [22, Definition 6], the permutation σ corresponds to an affine transformation of the monomial representation that preserves the polar code structure, making it an automorphism for polar codes following the standard partial order.[3]

By our assumption that $\{N-2, N-1\} \subseteq \mathcal{F}$, these positions are normally set to zero in the original codeword $\mathbf{c}^0$. However, under phase rotation, these positions take on specific values that uniquely identify the rotation angle:

$$\mathbf{c}^{\pi/2} : [u_{N-2}, u_{N-1}] = [1, 0], \tag{18}$$

$$\mathbf{c}^{\pi} : [u_{N-2}, u_{N-1}] = [0, 1], \tag{19}$$

$$\mathbf{c}^{3\pi/2} : [u_{N-2}, u_{N-1}] = [1, 1]. \tag{20}$$

These relationships enable integer phase ambiguity resolution by treating the last two frozen positions as information bits during decoding, then using the decoded values to determine the rotation angle.

B. Coherent Decoding for $\mathbf{x}_0$

The blind decoding architecture enables the receiver to estimate the channel without explicit pilots by treating the decoded codeword $\hat{\mathbf{c}}_1$ as an effective sequence of pilot symbols. Let $\hat{\mathbf{x}}_1$ denote the corresponding QPSK-modulated symbol vector. The receiver computes the maximum likelihood channel estimate as

$$\hat{h} = \frac{1}{N_c^1} \sum_{i=0}^{N_c^1 - 1} y_{1,i} \hat{x}_{1,i}^*, \tag{21}$$

[3]The permutation σ corresponds to affine transform $\mathbf{p} \mapsto \mathbf{A}\mathbf{p} + \mathbf{b}$ of vector of monomials $\mathbf{p} = [p_0, p_1, \ldots, p_{\log_2 N - 1}]$ with $\mathbf{A} = \mathbf{I}$ and $\mathbf{b} = [0, 0, \ldots, 0, 1]^\top$. The translation corresponds to flipping some message bits as per (18)-(20).

with estimation variance $\sigma_{\hat{h}}^2 = \sigma^2 / N_c^0$.

This channel estimate is then used for soft demodulation of the remaining data symbols. Specifically, for each bit k of symbol i, the receiver computes the log-likelihood ratio (LLR) as

$$\mathrm{LLR}_{i,k} = \log \frac{\sum_{x \in \mathcal{K}_{k,1}} \exp\left(-\frac{|y_{0,i} - \hat{h}x|^2}{\sigma_{\text{eff}}^2}\right)}{\sum_{x \in \mathcal{K}_{k,0}} \exp\left(-\frac{|y_{0,i} - \hat{h}x|^2}{\sigma_{\text{eff}}^2}\right)}, \tag{22}$$

where $\mathcal{K}_{k,0}$ and $\mathcal{K}_{k,1}$ denote the sets of constellation points with the k-th bit equal to 0 and 1, respectively, and $\sigma_{\text{eff}}^2 = \sigma_{\hat{h}}^2 + \sigma^2$ captures the aggregate uncertainty from both channel estimation and thermal noise. Armed with these bit-wise LLRs, the receiver proceeds with polar decoding to recover the information bits in $\mathbf{m}_0$.

V. Simulation Results

We evaluate performance over single block-fading channels with AWGN, comparing three schemes: pilot-aided transmission, genie-aided transmission (perfect channel knowledge), and the proposed code-splitting method.

A. Simulation Setup

We consider a block-fading channel where the channel coefficient $h = |h|e^{j\phi}$ has amplitude $|h| \sim \mathcal{U}(0.8, 1.2)$ and phase $\phi \sim \mathcal{U}(0, 2\pi)$, with $\mathcal{U}(a, b)$ denoting the uniform distribution over $[a, b]$. To enable a fair comparison across modulation orders, we fix the total number of channel uses for each scheme: 120 for QPSK, 60 for 16-QAM, and 40 for 64-QAM, matching the symbol rate and spectral efficiency of typical 5G NR control channel configurations [26].

In the pilot-aided baseline, we optimize pilot allocation by evaluating candidate values of 4, 8, 16, and 32 pilot symbols per packet. For each configuration, we determine the required SNR to achieve a block error rate (BLER) of 10^{-3}, and select the pilot length that minimizes this threshold. All schemes transmit $K = 120$ information bits per packet, with an 11-bit CRC for error detection as specified in the 5G NR standard [12]. Successive cancellation list (SCL) decoders with list size 8 are employed for all simulations.

For the proposed pilot-free communication framework, the parameters (N_c^1, K_1)—corresponding to the QPSK segment length and its assigned information bits—are set to $(16, 11)$ for QPSK, $(16, 27)$ for 16-QAM, and $(8, 14)$ for 64-QAM. Rate-matching and sub-block interleaving follow 5G NR recommendations. Figs 3 through 5 show BLER performance for each modulation order. For the optimized pilot-aided benchmarks, the selected numbers of pilot symbols N_p are 32 for QPSK, 16 for 16-QAM, and 8 for 64-QAM, respectively.

B. Performance Results

Figs. 3 through 5 illustrate the BLER performance for QPSK, 16-QAM, and 64-QAM, respectively. Across all cases, the proposed code-splitting architecture consistently achieves an approximate 1 dB coding gain relative to the pilot-aided benchmarks.

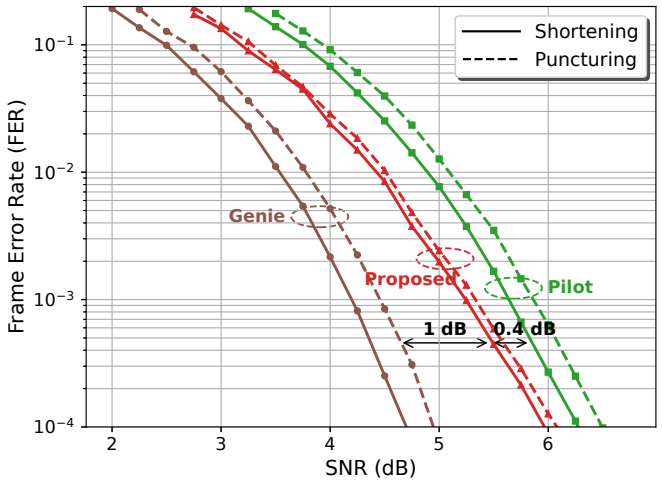

Fig. 3. BLER performance comparison for QPSK modulation with $K = 120$ information bits. The proposed method achieves approximately 0.4 dB gain over pilot-aided transmission.

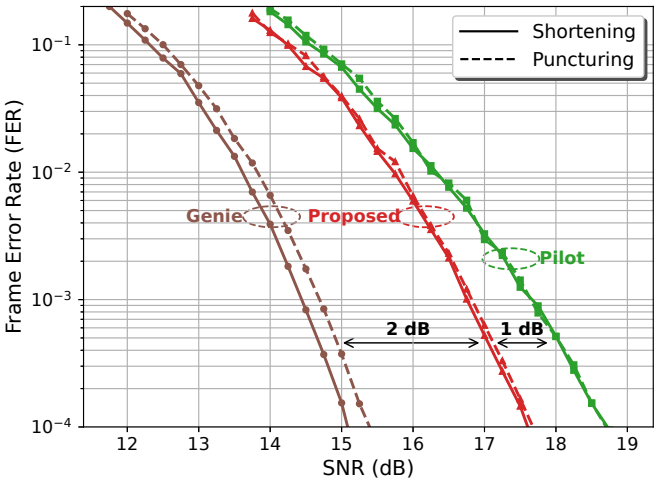

Fig. 5. BLER performance comparison for 64-QAM modulation with $K = 120$ information bits. The proposed method achieves approximately 1 dB gain over pilot-aided transmission.

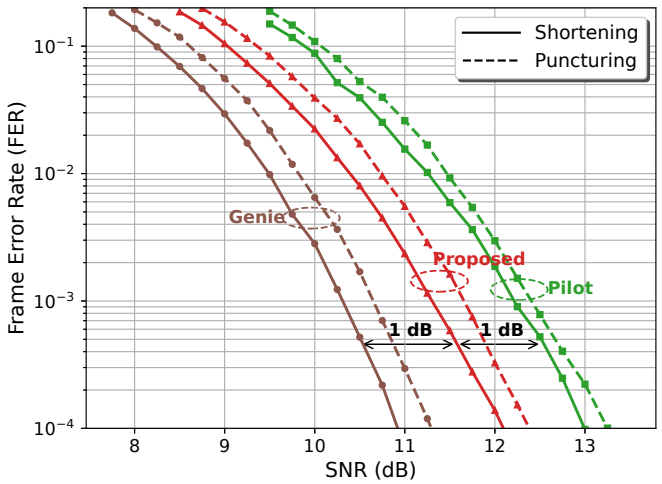

Fig. 4. BLER performance comparison for 16-QAM modulation with $K = 120$ information bits. The proposed method achieves approximately 1 dB gain over pilot-aided transmission.

This gain is attributed to two primary factors: first, the QPSK segment serves the dual role of carrying information and enabling channel estimation, thus eliminating the dedicated pilot overhead while preserving estimation accuracy. Second, the QAM portion benefits from a reduced code rate compared to the pilot-aided setup, which enhances its error correction capability. Together, these advantages translate into improved reliability and efficiency for short-packet transmission.

VI. Conclusion

This paper introduces a flexible pilot-free polar-coded transmission, breaking through the restrictions of prior methods by enabling both higher-order modulation and arbitrary codeword lengths. By leveraging a dual-structure architecture—where the QPSK segment simultaneously delivers data and enables blind channel estimation, and the QAM segment boosts spectral efficiency—the proposed scheme eliminates pilot overhead without sacrificing channel acquisition quality. Simulations show that this approach achieves up to 1 dB coding gain over conventional pilot-aided schemes, underscoring its potential for ultra-reliable low-latency short-packet applications where every symbol counts.

Looking ahead, promising directions include extending the framework to multi-block fading scenarios, optimizing the allocation of code-splitting resources, and evaluating robustness under practical channel conditions and hardware non-idealities.

References

[1] P. Popovski, K. F. Trillingsgaard, O. Simeone, and G. Durisi, "5G wireless network slicing for eMBB, URLLC, and mMTC: A communication-theoretic view," *IEEE Access*, vol. 6, pp. 55 765–55 779, 2018.

[2] L. Tong, B. Sadler, and M. Dong, "Pilot-assisted wireless transmissions: general model, design criteria, and signal processing," *IEEE Signal Process. Mag.*, vol. 21, no. 6, pp. 12–25, 2004.

[3] C.-X. Wang, X. You, X. Gao, X. Zhu, Z. Li, C. Zhang, H. Wang, Y. Huang, Y. Chen, H. Haas, J. S. Thompson, E. G. Larsson, M. D. Renzo, W. Tong, P. Zhu, X. Shen, H. V. Poor, and L. Hanzo, "On the road to 6G: Visions, requirements, key technologies, and testbeds," *IEEE Commun. Surveys Tuts.*, vol. 25, no. 2, pp. 905–974, 2nd Quart. 2023.

[4] K. David and H. Berndt, "6G vision and requirements: Is there any need for beyond 5G?" *IEEE Veh. Technol. Mag.*, vol. 13, no. 3, pp. 72–80, Sep. 2018.

[5] G. Durisi, T. Koch, and P. Popovski, "Toward massive, ultrareliable, and low-latency wireless communication with short packets," *Proceedings of the IEEE*, vol. 104, no. 9, pp. 1711–1726, 2016.

[6] J. Östman, G. Durisi, E. G. Ström, M. C. Coşkun, and G. Liva, "Short packets over block-memoryless fading channels: Pilot-assisted or noncoherent transmission?" *IEEE Trans. Commun.*, vol. 67, no. 2, pp. 1521–1536, 2019.

[7] L. Zheng and D. N. C. Tse, "Communication on the Grassmann manifold: A geometric approach to the noncoherent multiple-antenna channel," *IEEE Trans. Inf. Theory*, vol. 48, no. 2, pp. 359–383, 2002.

[8] J. Choi and N. Lee, "Generalized differential index modulation for pilot-free communications," *IEEE Internet Things J.*, vol. 8, no. 10, pp. 7973–7984, 2021.

[9] N. Lee, "Massive MIMO is very useful for pilot-free uplink communications," in *Proc. Inf. Theory Appl. Workshop (ITA)*, 2020.

[10] D. Han, B. Lee, M. Jang, D. Lee, S. Myung, and N. Lee, "Block orthogonal sparse superposition codes for L^3 communications: Low error rate, low latency, and low transmission power," *IEEE J. Sel. Areas Commun.*, vol. 43, no. 4, pp. 1183–1199, 2025.

[11] E. Arıkan, "Channel polarization: A method for constructing capacity-achieving codes for symmetric binary-input memoryless channels," *IEEE Trans. Inf. Theory*, vol. 55, no. 7, pp. 3051–3073, 2009.

[12] 3GPP, "NR; multiplexing and channel coding," *TS 38.212, Rel. 16*, 2020.

[13] I. Tal and A. Vardy, "List decoding of polar codes," *IEEE Trans. Inf. Theory*, vol. 61, no. 5, pp. 2213–2226, 2015.

[14] A. Balatsoukas-Stimming, M. B. Parizi, and A. Burg, "LLR-based successive cancellation list decoding of polar codes," *IEEE Trans. Signal Process.*, vol. 63, no. 19, pp. 5165–5179, 2015.

[15] K. Niu and K. Chen, "CRC-aided decoding of polar codes," *IEEE Commun. Lett.*, vol. 16, no. 10, pp. 1668–1671, 2012.

[16] P. Trifonov and V. Miloslavskaya, "Polar codes with dynamic frozen symbols and their decoding by directed search," in *Proc. IEEE Inf. Theory Workshop (ITW)*, 2013.

[17] T. Wang, D. Qu, and T. Jiang, "Parity-check-concatenated polar codes," *IEEE Commun. Lett.*, vol. 20, no. 12, pp. 2342–2345, Dec. 2016.

[18] E. Arıkan, "From sequential decoding to channel polarization and back again," *arXiv:1908.09594*, 2019, [Online]. Available: https://arxiv.org/abs/1908.09594.

[19] G. Choi and N. Lee, "Deep polar codes," *IEEE Trans. Commun.*, vol. 72, no. 7, pp. 3842–3855, 2024.

[20] ——, "Sparsely pre-transformed polar codes for low-latency SCL decoding," *IEEE Trans. Commun.*, 2025, early access.

[21] ——, "Rate-matching deep polar codes via polar coded extension," *arXiv:2505.06867*, 2025, [Online]. Available: https://arxiv.org/abs/2505.06867.

[22] M. Bardet, V. Dragoi, A. Otmani, and J.-P. Tillich, "Algebraic properties of polar codes from a new polynomial formalism," in *Proc. IEEE Int. Symp. Inf. Theory (ISIT)*, 2016, pp. 230–234.

[23] P. Yuan, M. C. Coşkun, and G. Kramer, "Polar-coded non-coherent communication," *IEEE Commun. Lett.*, vol. 25, no. 6, pp. 1786–1790, 2021.

[24] M. Geiselhart, M. Gauger, F. Krieg, J. Clausius, and S. T. Brink, "Phase-equivariant polar coded modulation," in *Proc. Int. Symp. on Topics in Coding (ISTC)*, 2023.

[25] G. Caire, G. Taricco, and E. Biglieri, "Bit-interleaved coded modulation," *IEEE Trans. Inf. Theory*, vol. 44, no. 3, pp. 927–946, 1998.

[26] 3GPP, "NR; physical channels and modulation," *TS 38.211, Rel. 16*, 2020.

[27] A. J. Viterbi and A. M. Viterbi, "Nonlinear estimation of PSK-modulated carrier phase with application to burst digital transmission," *IEEE Trans. Inf. Theory*, vol. 29, no. 4, pp. 543–551, 1983.

[28] F. Rice, M. Rice, and B. Cowley, "A new algorithm for 16QAM carrier phase estimation using qpsk partitioning," *Digital Signal Processing*, vol. 12, no. 1, pp. 77–86, 2002. [Online]. Available: https://www.sciencedirect.com/science/article/pii/S1051200401904002